



# A close-form solution for the maximum-power operating point of a solar cell array

S.M. Alghuwainem\*

*Department of Electrical Engineering, King Saud University, P.O. Box 800, Riyadh 11421, Saudi Arabia*

Received 21 March 1996; received in revised form 31 August 1996

---

## Abstract

A solar cell array is inherently a nonlinear device consisting of several solar cell modules connected in series-parallel combinations to provide the desired DC voltage and current. At a fixed insolation level, the terminal voltage decreases nonlinearly as the load current increases. Due to this nonlinearity, it is difficult to determine analytically the operating point at which the output power is maximum; a condition required for maximum utilization efficiency of the array. Iterative techniques are normally used to determine this operating condition. These techniques are lengthy, time-consuming, and have to be repeated for any change in the array's parameters, temperature, and insolation level. In this paper, an accurate closed-form solution is derived in terms of the array's parameters and solar insolation level. This solution is useful to the system designer or researcher as a fast and accurate tool for system design and performance analysis.

**Keywords:** Solar cell array; Matching to dc motor; Maximum power

---

## 1. Introduction

The use of photovoltaic (PV) power is increasingly spreading in the remote rural areas of many developing countries. The most successful application is to use a solar cell array to power a dedicated load such as a DC motor [1–4]. The key to their success is simplicity (direct coupling, no DC-AC conversion, no storage batteries, etc.). This arrangement is typically used on noncritical loads such as water pumps, which need not operate continuously and water can be used directly or stored easily.

---

\* Email: s.alghuwainem@ieee.org

A PV-powered DC motor can also be used to drive a three-phase self-excited induction generator [5, 6] to generate three-phase AC power. This arrangement is useful as part of an integrated renewable energy system (IRES), which takes advantage of the inherent diversity [7] of wind and solar insolation in most developing countries to improve power quality.

Due to the relatively high cost of a solar cell array, the main objective of the system designer is to extract maximum available electrical power output at all insolation levels, for maximum utilization efficiency of the system. The system consists of three separate devices; the array, the DC motor, and the mechanical load. Each device has its own characteristic which relates voltage and current (for an electrical device) or torque and speed (for a mechanical device). Since the DC motor is coupled directly to the array, both devices have the same operating voltage and current, and since the mechanical load is coupled to the shaft of the DC motor, both devices have the same speed. The torque required by the mechanical load depends on its torque speed characteristics. For example, a volumetric pump requires a constant torque at any speed, while a centrifugal pump requires a torque which is directly proportional to the square of the speed. Regardless of the type of mechanical load, an equilibrium steady-state operating point is reached where torque developed by the DC motor is sufficient to overcome the torque of the mechanical load plus frictional losses. This equilibrium operating point determines current, back emf, and terminal voltage of the motor. At a particular insolation level, there is a unique operating point (terminal voltage and current) on the PV array's characteristics at which power output is maximum. Therefore, for maximum utilization efficiency, it is necessary to match the three devices together such that the equilibrium operating point coincides with the maximum-power point of the solar cell array. However, since the maximum-power point varies with solar insolation during the day, and from season to season, it is difficult to maintain maximum-power operation at all insolation levels without changes in the system parameters. In order to overcome this problem, the system designer may either select a compromise matching, or use an electronic control device, known as a peak-power tracker (PPT), which continuously matches the array to the load. Ref. [8] is a comprehensive study of the starting and steady-state performance of several types of PV powered DC motors driving several types of water pumps. In [9], matching of DC motors to PV generators for maximum daily gross mechanical energy is reported. Peak-power tracking is achieved either by discretely interchanging the series-parallel connections of solar cell modules within the PV array [10], or by using a controlled DC-DC converter to adjust the voltage and current levels [11–13]. The technique presented in this paper enables the system designer to quickly predict the maximum-power operating point without resorting to lengthy, tedious, and time-consuming iterative techniques.

## **2. Characteristics of a solar cell array**

A solar cell array consists of several solar cell modules connected in series-parallel combinations to provide the desired voltage and current. The overall terminal

voltage, current, and internal resistance depend on the number of cells in series and the number of parallel strings. The  $I$ – $V$  characteristic equation of a single solar cell is often written as

$$V = \frac{1}{A} \ln \left( \frac{I_{ph} - \beta I - V/R_{sh} + I_0}{I_0} \right) - IR_s, \quad (1)$$

where  $V$  and  $I$  are cell terminal voltage and current, respectively;  $I_{ph}$  is photocurrent;  $I_0$  is diode reverse saturation current;  $R_s$  and  $R_{sh}$  are series and shunt resistance, respectively;  $\beta = 1 + R_s/R_{sh}$ ;  $A = q/kT$ ;  $q$  is the electron charge;  $k$  is the Boltzmann's constant;  $T$  is the absolute temperature; and  $A$  is the completion factor. It can be shown that the array parameters ( $a$  denotes array) of  $N$  identical cells are, for series array:

$I_{pha} = I_{ph}$ ,  $I_{0a} = I_0$ ,  $A_a = A/N$ ,  $R_{sa} = N R_s$ ,  $R_{sha} = N R_{sh}$ , and for parallel array:

$I_{pha} = N I_{ph}$ ,  $I_{0a} = N I_0$ ,  $A_a = A$ ,  $R_{sa} = R_s/N$ ,  $R_{sha} = R_{sh}/N$ .

The  $I$ – $V$  characteristic equation of an array may be written in the same form as that of a single cell as

$$V_a = \frac{1}{A_a} \ln \left( \frac{I_{pha} - \beta I_a - V_a/R_{sha} + I_{0a}}{I_{0a}} \right) - I_a R_{sa}. \quad (2)$$

Typical parameters for a single cell are:  $A = 13.7$  1/V,  $I_{ph} = 0.8$  A (at an insolation of  $1000$  W/m<sup>2</sup>),  $I_0 = 0.5$  mA,  $R_s = 0.05$   $\Omega$ , and  $R_{sh} = 10^5$   $\Omega$ . The array used in this study consists of 18 parallel strings, 324 cells in series per string, such that the array parameters are:  $A_a = 0.0422$  1/V,  $I_{pha} = 14.4$  A (at  $1000$  W/m<sup>2</sup> insolation),  $I_{0a} = 9$  mA,  $R_{sa} = 0.9$   $\Omega$ , and  $R_{sha} = 1.8$  M $\Omega$ . Fig. 1 is a plot of the array characteristics for different insolation levels.

It is clear from Fig. 1 that the array has different volt-ampere curves (one for each fixed insolation level). For each curve, the terminal voltage drops non-linearly as current is increased until it becomes zero at short-circuit. There is a unique intermediate point on each curve at which the product  $V_a I_a$  is maximum. The dashed line in Fig. 1 is the locus of such points for different insolation levels. For maximum utilization efficiency of the array, it is desirable to operate at the maximum-power point for all insolation levels. Therefore it is desirable that the operating point follows this line as the insolation varies during the day or from season to season.

### 3. Solving for maximum-power points

Power output from the array is given by

$$P_a = V_a I_a \quad (3)$$

For a specified set of array parameters  $A_a$ ,  $I_{pha}$ ,  $I_{0a}$ ,  $R_{sa}$ , and  $R_{sha}$ , the operating point ( $V_a$ ,  $I_a$ ), at which  $P_a$  is maximum must satisfy

$$\frac{dP_a}{dI_a} = 0. \quad (4)$$

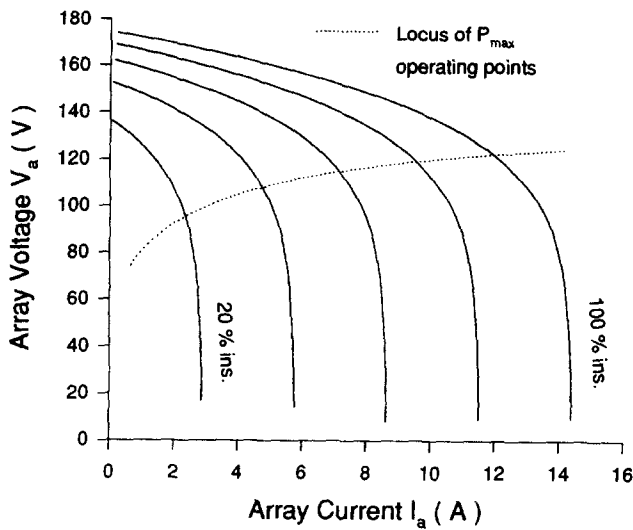


Fig. 1.  $V$ - $I$  characteristic of the solar cell array.

Eq. (4) may be written as

$$V_a + I_a \frac{dV_a}{dI_a} = 0. \quad (5)$$

Differentiating Eq. (2),

$$\frac{dV_a}{dI_a} = \frac{1}{A_a} \left( \frac{-(dV_a/dI_a)/R_{sha} - \beta}{I_{pha} - \beta I_a - V_a/R_{sha} + I_{0a}} \right) - R_{sa}. \quad (6)$$

The attempt to substitute Eq. (6) in Eq. (5) and solve for  $I_a$  did not lead to a close-form solution because of the presence of the term  $V_a/R_{sha}$ . However, since the objective of this paper is to seek a close-form solution, a simplified array model is used where it is assumed that  $V_a/R_{sha} \rightarrow 0$ . The error in using this simplified model is usually small for carefully designed cells, such that the calculated values are sufficiently accurate for engineering purposes. With this assumption, Eq. (6) becomes

$$\frac{dV_a}{dI_a} = \frac{1}{A_a} \left( \frac{-\beta}{I'_{pha} - \beta I_a + I_{0a}} \right) - R_{sa}, \quad (7)$$

where  $I'_{pha} = I_{pha} + I_{0a}$ . Therefore, Eq. (5) gives

$$\ln \left( \frac{I'_{pha} - \beta I_a}{I_{0a}} \right) - \frac{\beta I_a}{I'_{pha} - \beta I_a} - 2R_{sa}A_a I_a = 0. \quad (8)$$

Due to the presence of the logarithmic term, no close-form solution of Eq. (8) exists, and only a numerical solution is possible. Moreover, the numerical solution must be repeated for different values of array parameters ( $A_a$ ,  $I_{pha}$ ,  $I_{0a}$ ,  $R_{sa}$  and  $R_{sha}$ ). Eq. (8) is normally solved numerically using a gradient method such as the Newton–Raphson method or one of the equation solvers such as Mathcad [14].

#### 4. The proposed close-form solution

Eq. (8) is separated into two functions  $F_1$  and  $F_2$ , where

$$F_1 = \ln\left(\frac{I'_{pha} - \beta I_a}{I_{0a}}\right), \quad (9)$$

$$F_2 = \frac{\beta I_a}{I'_{pha} - \beta I_a} + 2R_{sa}A_a I_a. \quad (10)$$

Fig. 2 shows a plot of  $F_1$  and  $F_2$  versus  $I_a$  for  $I'_{pha} = 14.4$  A,  $I_{0a} = 0.009$  A,  $A_a = 0.0422$  1/V,  $R_{sa} = 0.9$   $\Omega$ , and  $R_{sha} = 1.8$  M $\Omega$

The point at which  $F_1$  and  $F_2$  intersect satisfies Eq. (8) and hence gives  $I_a$  at maximum power. However, it is clear from Fig. 2 that  $F_1$  is almost linear with respect to  $I_a$ , hence it can be approximated by a straight line to simplify the solution. This approximation is derived from the Taylor expansion of  $\ln(1+x)$  for  $x$  close

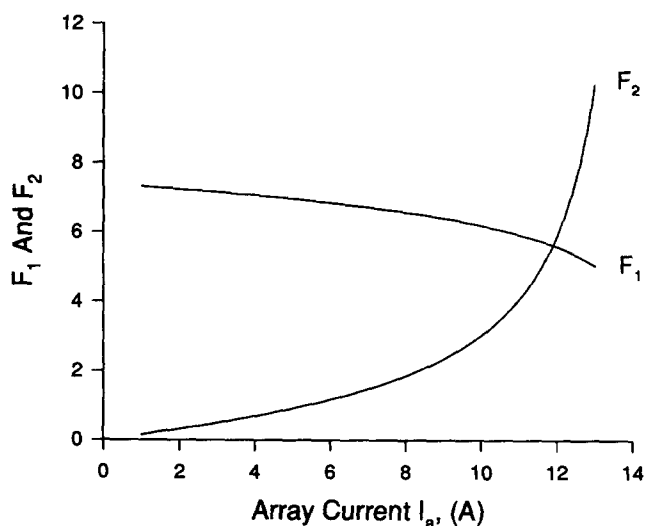


Fig. 2. Variation of  $F_1$  and  $F_2$  versus  $I_a$ .

to zero, as

$$\ln(1+x) = \sum_{n=1}^{\infty} (-1)^{n-1} \frac{(x)^n}{n}. \quad (11)$$

Taking the first term of Taylor expansion gives

$$\ln(1+x) \approx x \quad \text{for } x \approx 0. \quad (12)$$

$F_1$  is written as

$$F_1 = \ln\left(\frac{I'_{\text{pha}}}{I_{0a}}\right) + \ln\left(1 - \frac{\beta I_a}{I'_{\text{pha}}}\right) \quad (13)$$

$$\approx \ln\left(\frac{I'_{\text{pha}}}{I_{0a}}\right) - \frac{\beta I_a}{I'_{\text{pha}}}. \quad (14)$$

This approximation of  $F_1$  is simply a straight line having a slope of  $-\beta/I'_{\text{pha}}$ , and y-axis intercept of  $\ln(I'_{\text{pha}}/I_{0a})$ , as shown in Fig. 3.

It is clear from Fig. 3 that the approximate solution is not very accurate in this case. However, if the slope of the straight line is taken as  $-2\beta/I'_{\text{pha}}$ , a more accurate solution is obtained as shown in Fig. 4.

Therefore,  $F_1$  is approximated by

$$F_1 \approx \ln\left(\frac{I'_{\text{pha}}}{I_{0a}}\right) - 2 \frac{\beta I_a}{I'_{\text{pha}}}. \quad (15)$$

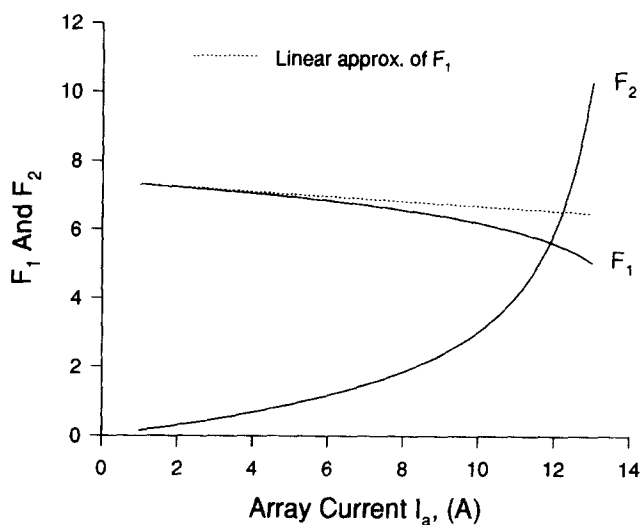


Fig. 3. Straight line approximation of  $F_1$ .

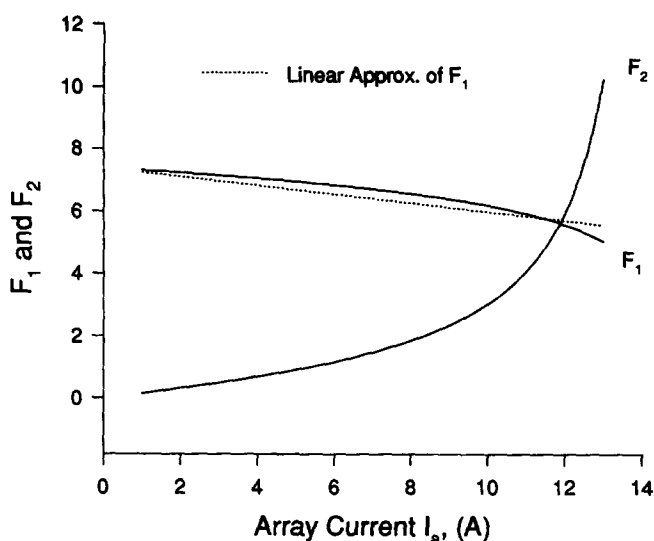


Fig. 4. Straight line approximation of  $F_1$  with increased slope.

Therefore, Eq. (8) becomes

$$\ln \left( \frac{I'_{pha}}{I'_{0a}} \right) - 2 \frac{\beta I_a}{I'_{pha}} - \frac{\beta I_a}{I'_{pha} - \beta I_a} - 2R_{sa}A_a I_a = 0. \quad (16)$$

Collecting terms, Eq. (16) may be written in the standard form of second order equation

$$aI_a^2 + bI_a + c = 0, \quad (17)$$

where

$$a = 2\beta^2 + 2\beta R_{sa}A_a I'_{pha} \quad (18)$$

$$b = I'_{pha}\beta \ln \left( \frac{I'_{pha}}{I'_{0a}} \right) - 3\beta I'_{pha} - 2R_{sa}A_a I'^2_{pha}, \quad (19)$$

$$c = I'_{pha} \ln \left( \frac{I'_{pha}}{I'_{0a}} \right). \quad (20)$$

It should be noted that coefficient  $a$  is dimensionless while  $b$  and  $c$  have the dimensions of current and current-squared, respectively, which is consistent with the dimensions of Eq. (17). Eq. (17) has two solutions, but only one is acceptable which gives  $I_a < I_{pha}$ , given by

$$I_a = \frac{1}{2a} [-b - \sqrt{b^2 - 4ac}]. \quad (21)$$

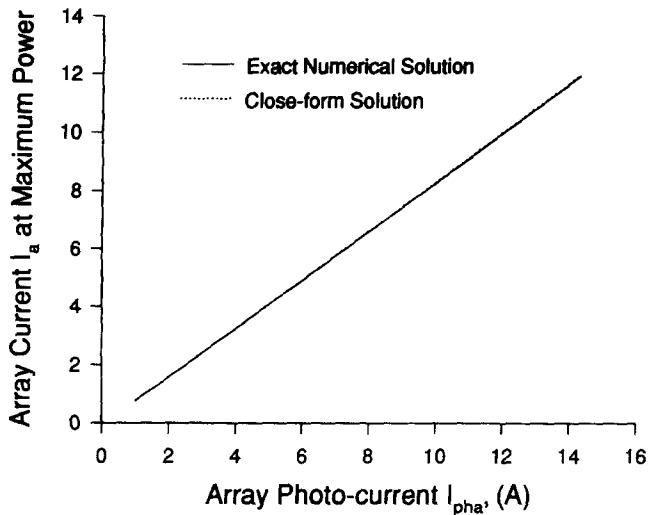


Fig. 5. Comparison of the close-form solution to exact numerical solution, for different values of photocurrent  $I_{pha}$ .

### 5. Accuracy of the close-form solution

The accuracy of the close-form solution is verified by comparing it with the exact numerical solution for different array parameters. Fig. 5 is a plot of the close-form solution and the exact numerical solution from which a very good agreement is observed.

### 6. Sensitivity to change in array parameters

Since a closed-form solution is obtained in terms of the coefficients  $a$ ,  $b$ , and  $c$ , it is only necessary to recalculate these coefficients. The new solution is then obtained by substituting the new coefficients in Eq. (21). Fig. 5 shows variation of the solution with variation in photocurrent  $I_{pha}$  while Fig. 6 shows the variation of the solution with  $A_a$ . It is clear from Figs. 5 and 6 that the accuracy of the close-form solution is not affected by changes in the array's parameters.

### 7. Conclusions

A simple and accurate close-form solution for the maximum-power operating point of a solar cell array is derived. The solution is useful for fast and accurate calculation of the maximum-power output conditions, without resorting to a lengthy,



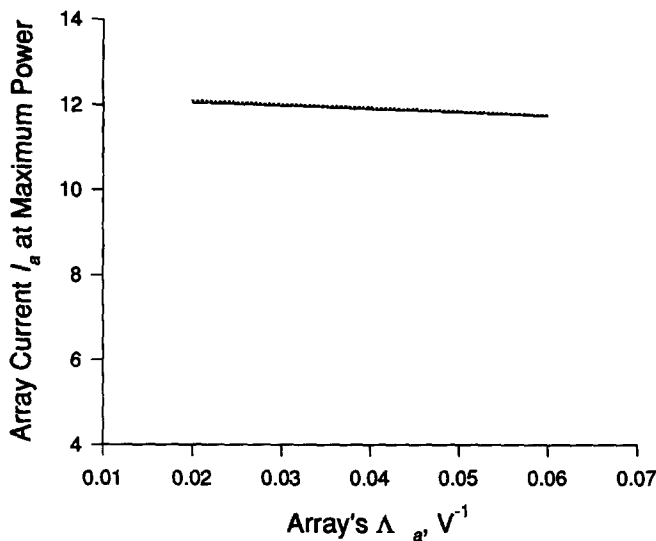


Fig. 6. Effect of array  $\Lambda$  on the accuracy of the close-form solution.

time-consuming iterative solution which has to be repeated for any change in array's parameters. The close-form solution is in the form of a simple formula with only three coefficients, in terms of the array parameters. Therefore, to repeat the solution due to change in array's parameters, it is only necessary to recalculate these coefficients and substitute in the close-form solution formula. The sensitivity of the maximum power operating point to changes in the array parameters can be easily studied using the close-form solution. It is found that the close-form solution is very accurate for all possible values of array parameters.

## References

- [1] J. Appelbaum, M.S. Sarma, IEEE Trans. Energy Conversion EC-4 (4) (1989) 635–642.
- [2] J. Appelbaum, IEEE Trans. Energy Conversion EC-4 (3) (1989) 351–357.
- [3] M.M. Saied, A.A. Hanafy et al., IEEE Trans. Energy Conversion EC-6 (4) (1991) 593–598.
- [4] S.M. Alghuwainem, IEEE Trans. Energy Conversion EC-7 (2) (1992) 267–272.
- [5] S.M. Alghuwainem, IEEE Trans. Energy Conversion 11 (1) (1996) 155–161.
- [6] S.M. Alghuwainem, IEEE Trans. Energy Conversion 11 (4) (1996) 768–773.
- [7] R. Ramakumar, IEEE Trans. Power Apparatus Systems PAS-102 (2) (1983) 502–510.
- [8] J. Appelbaum, IEEE Trans. Energy Conversion EC-1 (1) (1986) 17–25.
- [9] M.M. Saied, IEEE Trans. Energy Conversion EC-3 (3) (1988) 465–472.
- [10] Z. Zinger, A. Braunstein, IEEE Trans. Power Apparatus Systems PAS-100 (3) (1981) 1189–1192.
- [11] J.J. Schoeman, J.D. Van Wyk, IEEE Power Electron Specialist Conf. PESC-82, (1982) 361–367.
- [12] R. Hanitsch, R. Hauk, 6th E.C. Photovoltaic Solar Energy Conf. – Proc. Int. Conf. London, England, 1985.
- [13] S.M. Alghuwainem, IEEE Trans. Energy Conversion EC-9 (1) (1994) 192–198.
- [14] Mathcad User's Guide, MathSoft Inc., Cambridge, MA, 1994.